

A new blue light-emitting oligofluorene glass: synthesis, characterization and photophysical properties

Kevin D. Belfield,^{1*} Mykhailo V. Bondar,² Alma R. Morales,¹ Ozlem Yavuz¹ and Olga V. Przhonska²

¹Department of Chemistry, University of Central Florida, P.O. Box 162366, Orlando, Florida 32816-2366, USA

²Institute of Physics, Prospect Nauki 46, 03028 Kiev, Ukraine

Received 30 May 2002; revised 11 November 2002; accepted 13 November 2002

ABSTRACT: The synthesis, electrochemical, thermal and spectroscopic properties of the oligoaminofluorene derivative 9,9-didecyl-*N,N*-bis(9,9-didecyl-7-*N,N*-diphenylaminofluorene-2-yl)-*N,N*-diphenylfluorene-2,7-diamine (**4**), an organic glass, were investigated in solvents of differing polarity at room and 77 K temperature, including quantum yield and lifetime. The oligomer exhibited a glass transition near room temperature and was thermally stable to ca 400 °C. Intramolecular interactions between the fluorenyl chromophores were investigated. The relatively complex nature of the emission band of **4** was characterized by reduced anisotropy and two components in its fluorescence decay at room temperature. Emission spectra of **4** at 77 K exhibited a single component in its fluorescence decay and a dependence on the excitation wavelength at the red edge of the absorption band. A spectroscopic model of **4** is proposed to explain the observed spectral behavior of this potentially important electroluminescent material. Copyright © 2003 John Wiley & Sons, Ltd.

KEYWORDS: oligofluorene derivative; fluorescence; excitation anisotropy; organic glass

INTRODUCTION

Chromogenic organic materials are of significant interest owing to their numerous scientific and technological applications,^{1–3} including light-emitting diodes (LEDs),² fluorescent probes, two-photon absorption and optical limiting devices.³ Electroluminescence, light emission resulting from the application of an electric field, in organic materials is being harnessed in current LED-based displays, sensors and indicators. The excitation leading to luminescence is accomplished by recombination of charge carriers of opposite sign (electron and hole) injected into an inorganic or organic semiconductor in the presence of an external electrical circuit. Since the first report of electroluminescence in an organic material, anthracene, in 1963, and subsequent reports of electroluminescence in a polymer, poly(phenylenevinylene), numerous organic materials and polymers have been reported over the past decade for use as organic light-emitting diodes (OLEDs) or polymer light-emitting diodes (PLEDs).⁴

Organic polymer LEDs have a number of advantages for the development of large-area LED displays because of their potentially good processability, low operating voltage, fast response time and color tunability over the entire visible spectral range by control of the HOMO–LUMO band gap of the emissive material. Conjugated polymers are semiconductors, the semiconducting behavior being associated with the π molecular orbitals that are delocalized along the polymer chain. Their primary advantage over non-polymeric organic materials is the possibility of processing the polymer through melt processing or solution casting to form robust conformal structures. High molar mass organic glasses may also bear this advantage but are relatively uncommon. For the use of these materials in OLEDs as, e.g., hole-transport layers or emissive layers, they should possess a wide variety of physical properties, including electrochemical stability, low ionization potential, reversible redox behavior, hole-transport and injection ability. In addition, they should exhibit high thermal and photochemical stability, be soluble and possess the ability to form good films.

The progress in the performance of OLEDs and PLEDs has been impressive. The colors emitted by current materials nearly span the entire visible range, although relatively few stable materials have been found that emit blue light. Hence stable blue light-emitting organic materials and polymers remains an area of active investigation, since stable, efficient and high-brightness blue light-emitting materials are particularly desirable for

*Correspondence to: K. D. Belfield, Department of Chemistry, University of Central Florida, P.O. Box 162366, Orlando, Florida 32816-2366, USA.

E-mail: kbelfiel@mail.ucf.edu

Contract/grant sponsor: Petroleum Research Fund.

Contract/grant sponsor: Research Corporation.

Contract/grant sponsor: National Science Foundation; Contract/grant number: DMR-9975773; Contract/grant number: ECS-9970078;

Contract/grant number: ECS-9976630.

Contract/grant sponsor: National Research Council (COBASE).

Contract/grant sponsor: University of Central Florida.

full color displays. Blue light can be used to generate longer wavelengths with the proper selection of dyes through energy transfer to lower energy fluorophores. Hence not only are blue light-emitting materials an important component for multicolor LED displays, but also a blue LED can, in principle, generate all the colors necessary for a display.⁴

Polyfluorene derivatives are of particular interest owing to their efficient photoluminescence and electroluminescence properties. Purity is of paramount importance for good electroluminescent performance since impurities can act as quenching sites. Thus, well-defined fluorenyl oligomers may be preferable to polymers owing to the ease of purification and ability to synthesize discrete, defect-free molecular structures. Molecules with covalently linked chromophores allow the investigation of processes involving chromophore interactions manifested in the nature of absorption bands,⁵ fluorescence efficiency⁶ and other characteristics of spectral behavior.⁷ Relatively little is known about chromophore–chromophore interactions in compounds containing multiple fluorene units, and a well-defined fluorenyl oligomer would be ideal to probe such interactions. In addition, fluorene derivatives known to have high two-photon absorptivity⁸ and good thermal and photochemical stability^{9,10} are being investigated for a number of applications where an understanding of their photophysical behavior is critical.

In order to understand more fully the electronic nature and design of new fluorene-based luminescent materials, we have investigated the photophysical properties of a number of fluorene derivatives.^{11,12} Here, we report the synthesis, characterization and electrochemical and spectroscopic measurements of an amorphous oligofluorene derivative, 9,9-didecyl-*N,N*-bis(9,9-didecyl-7-*N,N*-diphenylamino)fluorene-2-yl)-*N,N*-diphenylfluorene-2,7-diamine (**4**), designed specifically to probe chromophore interactions. Fluorescence lifetimes in solvents of varying polarity (at room temperature and 77 K) and quantum yields (at room temperature) were determined. The fluorenyl ring system was chosen as a thermally and photochemically stable π -conjugated system that can be readily functionalized at the 2- and/or 7-positions. Alkylation of the 9-position can modulate solubility and, perhaps, chromophore–chromophore interactions. The solid-state luminescence spectrum along with electrochemical and thermal properties of **4** are reported.

EXPERIMENTAL

General. 9,9-Didecyl-2,7-diiodofluorene (**1**) was prepared as described previously.⁸ Reactions were conducted under an N₂ atmosphere. Aniline was distilled under reduced pressure prior to use. All other reagents and solvents were used as received from commercial suppliers. ¹H and ¹³C NMR spectra were recorded in

CDCl₃ or C₆D₆ on Varian 300 Mercury NMR spectrometers at 300 MHz. FT-IR spectra were recorded on a Perkin-Elmer Spectrum One spectrophotometer.

General procedure for the Ullmann condensation used for the preparation of oligofluorene 4 and its precursors 2 and 3. *N*-(9,9-Didecyl-7-iodofluorene-2-yl)-*N,N*-diphenylamine (**2**): 9,9-didecyl-2,7-diiodofluorene (**1**) (1.22 g, 1.7 mmol) was dissolved in 6 ml of 1,2-dichlorobenzene at room temperature under N₂. To this were added K₂CO₃ (1.90 g, 13.77 mmol), 18-crown-6 (0.15 g, 0.61 mmol) and copper bronze (0.53 g, 8.32 mmol) at room temperature. *N,N*-Diphenylamine (0.30 g, 1.77 mmol) was added and the reaction mixture was heated at 180 °C for 28 h. Upon completion, the brown mixture was filtered through a short silica gel plug and the yellow solution was concentrated, resulting in a yellow–brown oil. 1,2-Dichlorobenzene was removed under reduced pressure. Purification was accomplished by column chromatography using first hexanes–CH₂Cl₂ (80:20), followed by hexanes–CH₂Cl₂ (90:10), providing 0.44 g of white solid (mp = 53–54 °C) (35%). ¹H NMR (300 MHz, CDCl₃), δ (ppm): 7.61 (d, 2H), 7.52 (d, 1H), 7.35 (d, 1H), 7.22 (t, 5H), 7.12 (t, 5H), 7.03 (t, 2H), 1.81 (m, 4H), 1.11 (m, 28H), 0.86 (t, 6H), 0.62 (bs, 4H). ¹³C NMR (300 MHz, CDCl₃), δ (ppm): 153.3, 151.7, 148.1, 147.9, 140.8, 136.0, 135.0, 132.0, 129.4, 124.1, 123.6, 122.8, 121.0, 120.7, 119.2, 91.7, 55.4, 40.3, 32.1, 30.1, 29.8, 29.8, 29.5, 24.0, 22.9, 14.3. FT-IR (KBr, cm⁻¹): 3032 (ν ArCH), 2923, 2851 (ν AlCH), (ν ArC=C).

9,9-Didecyl-2,7-bis(*N*-phenylamino)fluorene (3). 9,9-Didecyl-2,7-diiodofluorene and aniline were subjected to Ullmann condensation conditions as reported above. A yellow–brown oil was obtained after column chromatographic purification using first *n*-hexane–EtOAc (80:20), followed by *n*-hexane–EtOAc (95:5) (0.40 g, 45% yield). UV–visible (acetonitrile): λ_{max} = 354 nm (250–400 nm). Anal. Calcd for C₄₅H₆₀N₂: C, 85.93, H, 9.62, N, 4.45. Found: C, 85.91, H, 9.62, N, 4.45%. ¹H NMR (300 MHz, CDCl₃), δ (ppm): 7.49 (s, 2H), 7.24 (d, 4H), 7.05 (d, 8H), 6.91 (s, 2H), 5.7 (bs, 2H), 1.88 (bs, 4H), 1.11 (m, 28H), 0.84 (m, 10H). FT-IR (KBr, cm⁻¹): 3397 (ν NH), 3031 (ν ArCH), 2923, 2855 (ν AlCH), 1598 (ν ArC=C).

9,9-Didecyl-*N,N*-bis(9,9-didecyl-7-*N,N*-diphenylamino)fluorene-2-yl)-*N,N*-diphenylfluorene-2,7-diamine (4). *N*-(9,9-Didecyl-7-iodofluorene-2-yl)-*N,N*-diphenylamine (**2**) (0.49 g, 0.66 mmol) was subjected to a similar Ullmann condensation reaction with 9,9-didecyl-2,7-bis(*N*-phenylamino)fluorene (**3**) (0.17 g, 0.27 mmol), as reported above, to yield the desired product **4**. TLC analysis [hexanes–CH₂Cl₂ (60:40)] indicated that condensation was complete after 4 days. The orange–brown oil was further purified by column chromatography on silica gel using first hexanes–CH₂Cl₂ (70:30) followed by hexanes–CH₂Cl₂ (80:20), resulting in 0.42 g of yellow solid

(85% yield). Anal. Calcd for $C_{135}H_{174}N_4$: C, 87.51, H, 9.46, N, 3.02. Found: C, 87.37, H, 9.53, N, 3.02%. 1H NMR (300 MHz, C_6D_6), δ (ppm): 7.09 (d, 2H), 7.04 (s, 1H), 7.0 (dd, 5H), 6.93 (s, 1H), 6.85 (t, 6H), 6.73 (t, 6H), 6.53 (m, 3H), 1.33 (m, 4H), 0.87 (bd, 28 H), 0.52 (bt, 10H). ^{13}C NMR (300 MHz, C_6D_6), δ (ppm): 152.4, 148.5, 147.0, 136.6, 129.4, 124.2, 123.9, 120.2, 119.6, 119.1, 55.2, 40.3, 32.2, 30.4, 30.0, 29.8, 29.7, 29.6, 24.4, 22.9, 14.2. FT-IR (KBr, cm^{-1}): 3036 (ν_{ArCH}), 2926, 2854 (ν_{AlCH}), 1593 ($\nu_{ArC=C}$).

Techniques. All electrochemical characterizations were studied with an EG&G Princeton Applied Research Model 273 potentiostat/galvanostat. Electrochemical experiments were carried out in tetrabutylammonium hexafluorophosphate (TBAHFP₄) (Fluka) in CH_2Cl_2 solution (HPLC grade) (Fischer Scientific). All solutions were bubbled with nitrogen for 20 min prior to the experiments. The working and counter electrodes were a platinum (Pt) wire. In all cases, silver wire coated with silver chloride was used as a reference electrode. The potential of this electrode was 450 mV vs ferrocene or 40 mV vs SCE. All potentials given refer to this reference electrode. Concentration of the compounds used were 3×10^{-4} M in each case and the electrolyte was 0.1 M TBAHFP₄.

Thermal stability was assessed by thermogravimetric analysis (TGA) with a TA Instruments Model 2050 instrument under N_2 at a heating rate of $20^\circ C \text{ min}^{-1}$ from room temperature to $550^\circ C$. Phase and glass transitions were investigated by differential scanning calorimetry (DSC) using a TA Instruments Model 2920 instrument, at heating/cooling rates of $10^\circ C \text{ min}^{-1}$ under N_2 .

Steady-state absorption, fluorescence, excitation and excitation anisotropy spectra were investigated for **4** in hexane, THF, CH_2Cl_2 and silicone oil (viscosity ~ 200 cP at $25^\circ C$) at room temperature and in 2-methyltetrahydrofuran (Me-THF) at 77 K. All solvents used in these experiments were checked for spurious emission in the region of interest and purged with nitrogen for 20 min before use. Absorption spectra were measured with a Cary-3 UV-visible spectrophotometer. Steady-state fluorescence, excitation and excitation anisotropy spectra at room temperature and 77 K were obtained with a PTI Quantmaster spectrofluorimeter. Fluorescence lifetimes were measured with a PTI Timemaster spectrofluorimeter with a strobe photomultiplier tube and 600 ps dye laser, tunable in the spectral region 370–400 nm (Model GL 302). The time resolution of the system based on the software processing of experimental data did not exceed 100 ps, checked by fluorescence picosecond lifetime measurements for the standard 4-dimethylamino-4'-cyanostilbene (DCS).¹⁰ All experimental data at room temperature were obtained with 10 mm quartz cuvettes and with special cryostat quartz tubes at 77 K. The concentrations for the investigated solutions did not exceed 5×10^{-6} M, and processes of reabsorption were

negligible. Excitation anisotropy spectra were measured by the T-format method with correction for background signals.¹³ Quantum yields, Φ , were calculated from the corrected fluorescence spectra by a standard method,¹³ relative to Rhodamine 6G in ethanol ($\Phi \approx 0.94$).¹⁴

RESULTS AND DISCUSSION

A versatile fluorene-based intermediate, **1**, was used for the preparation of two key intermediates, fluorene derivatives **2** and **3** (Fig. 1). Ullmann condensation reaction of diarylamines with iodinated aromatic compounds was utilized to provide access to a number of fluorene analogs in reasonable yield. The Ullmann reactions were conducted with K_2CO_3 as base, 18-crown-6 and copper bronze in 1,2-dichlorobenzene under N_2 at reflux.⁸ Iodofluorene derivative **2** was isolated in 38% yield as a white solid. The FT-IR, 1H and ^{13}C NMR spectra provided structural confirmation of **2**. The bis(*N*-phenylamino)fluorene derivative **3** was obtained by reaction of **1** with aniline in 45% yield as a fluorescent yellow viscous oil. The FT-IR spectrum of **3** revealed characteristic stretching absorptions for NH (3397 cm^{-1}). CHN analysis was in excellent agreement with the calculated values.

The versatility of the Ullmann condensation reaction was demonstrated in the formation of a new dye, the oligofluorene **4** [Fig. 2(a)]. The structure of this chromophore is based on a symmetrical molecule consisting of three fluorenyl ring systems separated by aminophenyl moieties, flanked by bisdiphenylamino π electron donor groups. Hence **2** was subjected to similar Ullmann amination conditions with fluorene **3**, providing oligofluorene **4** in good yield (85%). CHN analysis was in excellent agreement with the calculated values, and the FT-IR spectrum revealed the complete disappearance of the NH stretching vibrations. 1H and ^{13}C NMR spectroscopic data provided additional structural confirmation of **4**.

Thermal analyses were performed on **4** to ascertain its

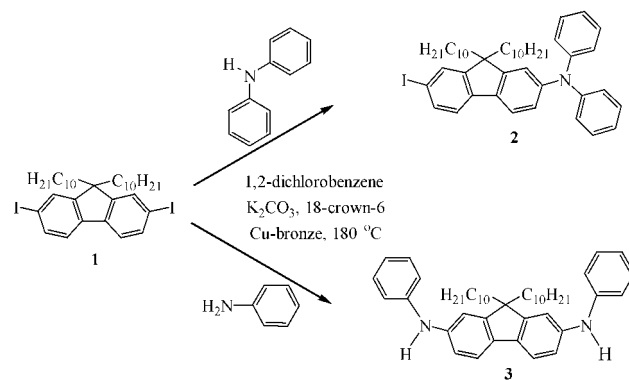


Figure 1. Synthesis of precursors **2** and **3** via Ullmann condensation reactions

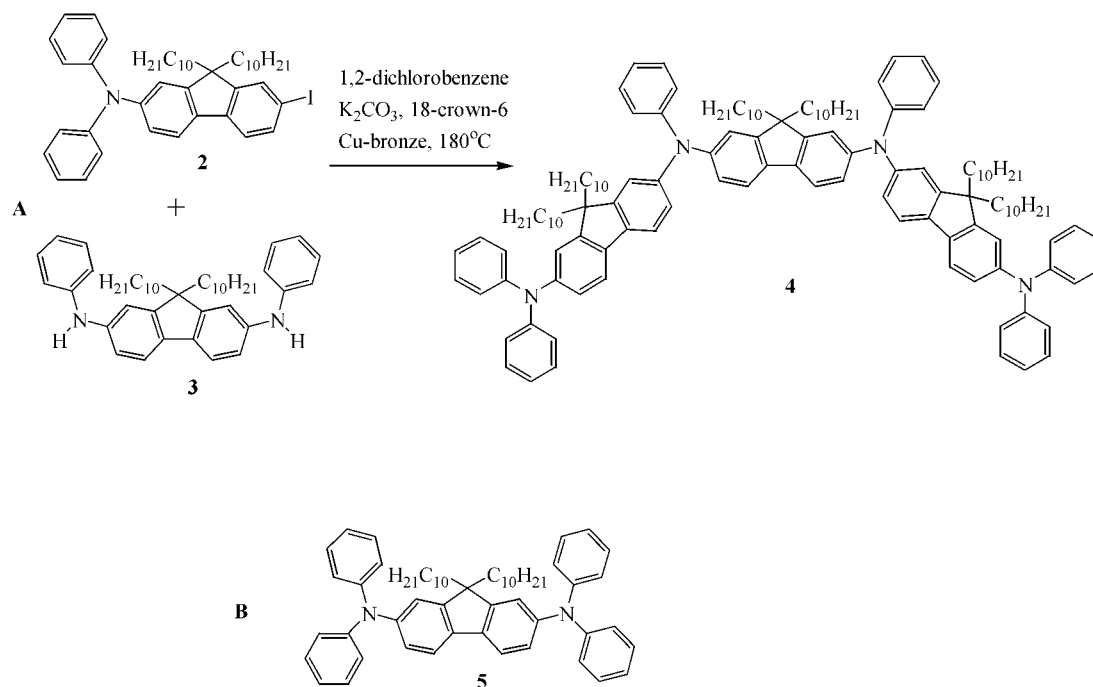


Figure 2. (a) Synthesis of symmetrical oligofluorene **4** containing three non-conjugated fluorenyl rings, and (b) structure of 9,9-didecyl-2,7-bis(*N,N*-diphenylamino)fluorene (**5**)

thermal stability and properties. TGA analysis, performed under N_2 at a heating rate of $20^\circ C \text{ min}^{-1}$ from room temperature to $550^\circ C$, revealed **4** to exhibit high thermal stability up to $395^\circ C$ (2% weight loss). A weight loss of 48% was subsequently observed between 395 and $550^\circ C$, leaving a residue corresponding to 50% of the original sample weight. Repeated DSC scans with controlled heating and cooling were performed on **4** at a rate of $10^\circ C \text{ min}^{-1}$ under N_2 . No melting or crystallization transitions were detected between -40 and $325^\circ C$. The DSC analysis revealed a glass transition, T_g , onset at $20^\circ C$ and T_g midpoint at $24^\circ C$. Controlled cooling revealed an obvious transition from 24 to $19^\circ C$ that correlated with the T_g observed during the heating scan. The DSC analysis indicated that **4** is amorphous and behaves like a glassy material in which no melting or crystallization transitions are observed. Although the low T_g precludes the use of neat **4** at room temperature, inclusion of **4** in a guest–host system with a high- T_g polymer may be a suitable alternative.¹⁵

The cyclic voltammetric (CV) curves for oligofluorene derivative **4** and the corresponding model compound 9,9-didecyl-2,7-bis(*N,N*-diphenylamino)fluorene (**5**) are presented in Fig. 3. These compounds exhibited relatively low and highly reversible oxidation and reduction potentials in CH_2Cl_2 , which can be assigned to the formation of the different cation radicals in solution. Fluorene **5** displayed two sequential oxidations in CH_2Cl_2 [Fig. 3(a)]. This derivative underwent reversible oxidations and reductions, allowing for the calculation of the ionization potentials. The first and second ionization

potentials for fluorene **5** were 4.89 and 5.23 eV, respectively. The first and second oxidation potentials were 0.488 and 0.826 V, respectively, with corresponding reduction potentials of 0.404 and 0.718 V, respectively. Repeated cycling did not cause any appreciable change in the shape or height of the CV waves and no deposition was observed on the Pt electrode.

Oligofluorene **4** revealed two reversible and one quasi-reversible anodic (oxidation) peaks at 0.428, 0.634 and 1.002 V with corresponding cathodic (reduction) peaks at 0.396, 0.580 and 0.834 V, respectively, in CH_2Cl_2 [Fig. 3(b)]. The ionization potentials were calculated as 4.86, 5.03 and 5.40 eV. *In situ* UV–visible spectral analysis of **4** and **5** revealed a sharp absorption with a maximum at 480 nm upon the first oxidation, consistent with formation of a cation radical.¹⁶ The CV results demonstrate the relative ease of oxidation of oligofluorene **4** (formation of the cation radical and low oxidation potentials) and its high apparent electrochemical stability.

The oligofluorene **4** [Fig. 2(a)] represents a symmetrical molecule with three non-conjugated, covalently linked fluorenyl rings. The structure of the central chromophore corresponds to the 9,9-didecylfluorene unit, which in monomeric form is characterized by the main absorption maximum $\lambda^{\text{max}} \approx 300 \text{ nm}$.³ The end chromophores are very similar to the symmetrical compound 9,9-didecyl-2,7-bis(*N,N*-diphenylamino)fluorene (**5**) [Fig. 2(b)] with $\lambda^{\text{max}} \approx 375 \text{ nm}$.¹¹ We can assume that the absorption bands of non-symmetrical end chromophores in the non-conjugated covalently linked compound **4** should be shifted to the long-wavelength region relative

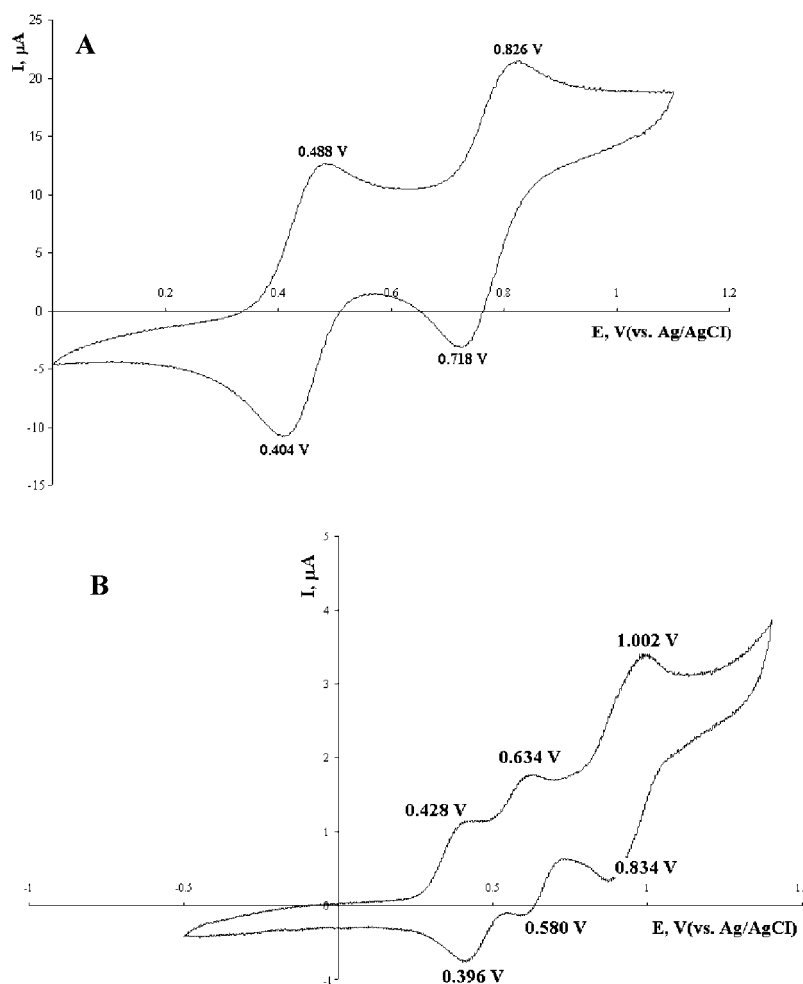


Figure 3. Cyclic voltammogram of (a) **5** and (b) **4** in CH_2Cl_2 . Scan rate, 50 mW s^{-1} ; reference electrode, Ag/AgCl

to the corresponding absorption band of the separate symmetric molecule **5** with $\lambda^{\text{max}} \approx 375 \text{ nm}$. Therefore, we can roughly present the absorption band of the entire molecule **4** with $\lambda^{\text{max}} \approx 397 \text{ nm}$ as a simple summing of the absorption spectra of all covalently linked chromophores in **4**. Quantum chemical calculations for similar fluorene derivatives (AF50 and AF210) also confirmed a weak sensitivity of λ^{max} for these compounds to the number of non-conjugated fluorene groups contained within the molecule.¹⁷

Absorption, fluorescence and excitation anisotropy spectra of **4** in silicone oil, hexane, THF and CH_2Cl_2 at room temperature are presented in Fig. 4(a). The absorption and emission spectra exhibited a weak dependence on the solvent polarity, $\Delta f = [(e - 1)/(2e + 1)] - [(n^2 - 1)/(2n^2 + 1)]$, where e and n are the dielectric constant of the solvent and its refractive index, respectively,¹³ while the Stoke's shift increased slightly with Δf . Extinction coefficients for compounds **4**, $\varepsilon_1^{\text{max}}$, and **5**, $\varepsilon_2^{\text{max}}$, are presented in Table 1. From these data, it can be seen that doubling the number of fluorene groups absorbing near λ^{max} (end chromophores in **4**) triples the

$\varepsilon_1^{\text{max}}$ of **4** in hexane and THF. The same tendency was observed for AF210 in comparison with AF50 in THF.¹⁷ In general, the extinction coefficient is a complex function of the molecular structure but it roughly scales with the number of fluorenyl units for oligofluorene **4**.

The room temperature fluorescence spectra of fluorene **4** [Fig. 4(a), curves 5–7], in all of the solvents investigated, were independent of the excitation wavelength, λ_{exc} , over the entire absorption band. The value of excitation anisotropy, r , of **4** was relatively high in viscous silicone oil (curve 8), and constant only at the red edge of the absorption band ($\lambda_{\text{exc}} \geq 400 \text{ nm}$). This behavior is in contrast to that of compound **5**, which exhibited nearly the same anisotropy over the entire primary absorption band [Fig. 4(b), curve 2]. A decrease in anisotropy was observed for $\lambda_{\text{exc}} \leq 340 \text{ nm}$, corresponding to the second electronic transition of **5**. Fluorescence lifetime measurements of **4** revealed two components in the fluorescence decay, τ_1 , and τ_2 , upon excitation in the blue edge of the absorption band. The amplitudes of these components were comparable to each other, which cannot be explained by emission from

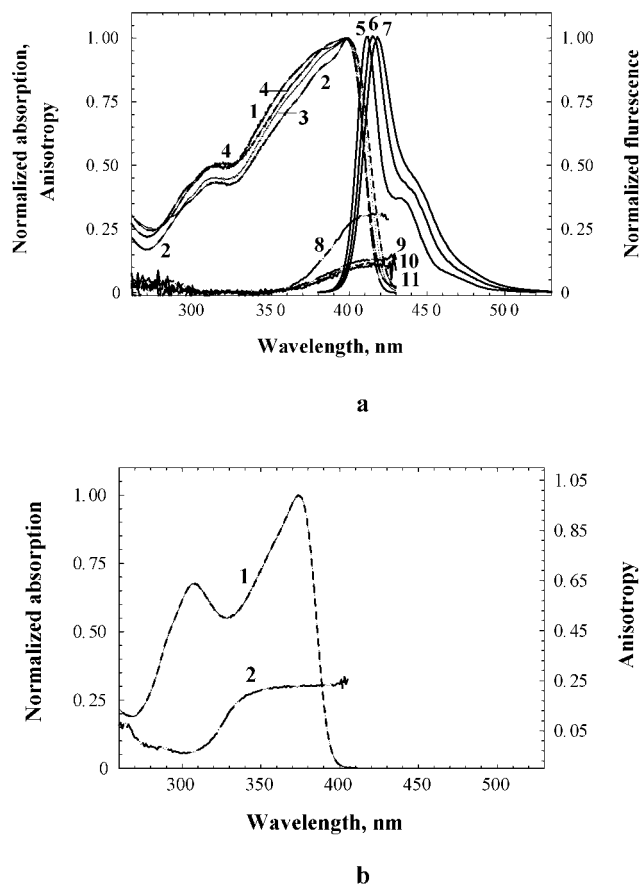


Figure 4. (a) Normalized absorption (1–4), fluorescence (5–7) and excitation anisotropy (8–11) spectra for **4** in silicone oil (1, 8), hexane (2, 5, 9), THF (3, 6, 10) and CH_2Cl_2 (4, 7, 11). (b) Normalized absorption in THF (1) and excitation anisotropy in silicone oil (2) for **5** (observation wavelength, $\lambda_{\text{obs}} \approx 415$ nm)

impurities. The lifetimes are presented in Table 1 along with goodness-of-fit parameter χ^2 .

The spectral peculiarities (two lifetime components and anisotropy) observed for oligofluorene **4** at room temperature can be explained by the spectroscopic model presented in Fig. 5. Assuming that the absorption spectrum of **4** roughly corresponds to the two different conformers of **4** which exist in thermodynamic equilibrium in the ground state, these conformers can be characterized by electronic levels S_0 , S_1 , S_2 and S'_0 , S'_1 , S'_2 , respectively. Excited electronic levels S_2 and S'_2 most likely correspond to the charge localization at the central chromophore with absorption maximum $\lambda_{\text{max}}^{\text{max}} \approx 340\text{--}360$ nm. The excited-state energy levels S_1 and S'_1 ($\lambda_{\text{max}}^{\text{max}} \approx 390\text{--}400$ nm) are close to each other and correspond to the charge localization at the end chromophores with different space orientation relative to the central fluorene moiety.

One can imagine, e.g., that electronic level S'_1 belongs to the chromophore with a parallel orientation of the molecular axis, but level S_1 corresponds to a form with the molecular axis rotated relative to the central chromophore. After the excitation to S_1 , this chromophore orientation becomes unstable and quickly relaxes to the more energetically preferable configuration, S'_1 , with the corresponding velocity $k_{11'}$. The emission spectra from S'_1 (long wavelength emitting) and S_1 (short wavelength emitting) are also close but characterized by different lifetimes ($\tau_1 \approx 0.9\text{--}1.3$ ns; $\tau_2 \approx 0.1\text{--}0.2$ ns). Thus, the steady-state fluorescence spectrum of **4** corresponded primarily to emission of the longer wavelength chromophore, independent of excitation wavelength at room temperature. A low value of anisotropy for $\lambda_{\text{exc}} < 400$ nm is associated with different orientations of the transition dipole moments $S_0 \rightarrow S_1$ and $S'_1 \rightarrow S'_0$ relative to the central fluorene moiety. For $\lambda_{\text{exc}} \geq 400$ nm, the anisotropy increased, which can be

Table 1. Spectroscopic parameters of compounds **4** and **5** using different solvents: maximum of the absorption, $\lambda_{\text{a}}^{\text{max}}$, and emission, $\lambda_{\text{e}}^{\text{max}}$, wavelengths; extinction coefficients, ϵ_1^{max} and ϵ_2^{max} , at $\lambda_{\text{a}}^{\text{max}}$; quantum yields, Φ_1 and Φ_2 ; lifetimes, τ_1 , τ_2 and τ , for **4** and **5**

Compound	Parameter	Silicone oil	Hexane	THF	CH_2Cl_2	Me-THF, 77 K
4	$\lambda_{\text{a}}^{\text{max}}$ (nm)	397	398	398	397	—
	$\lambda_{\text{e}}^{\text{max}}$ (nm)	—	412	415	418	—
	$\epsilon_1^{\text{max}} \times 10^{-3}$ ($\text{l mol}^{-1} \text{cm}^{-1}$)	—	117 ± 10	103 ± 10	64 ± 7	—
	τ_1^{a} (ns)	0.95 ± 0.06	1.05 ± 0.1	1.25 ± 0.15	1.3 ± 0.15	1.55 ± 0.1
	τ_2^{a} (ns)	0.1 ± 0.1	0.15 ± 0.05	0.1 ± 0.03	0.11 ± 0.02	—
	χ_2^2	1.02	1.05	1.1	1.05	1.05
	Φ_1	—	1.0 ± 0.05	1.0 ± 0.05	0.95 ± 0.05	—
5	$\lambda_{\text{a}}^{\text{max}}$ (nm)	—	375	374	374	—
	$\lambda_{\text{e}}^{\text{max}}$ (nm)	—	390	395	397	—
	$\epsilon_2^{\text{max}} \times 10^{-3}$, ($\text{l mol}^{-1} \text{cm}^{-1}$)	—	44 ± 5	30 ± 3	37 ± 4	—
	Φ_2	—	0.4 ± 0.05	0.5 ± 0.08	0.15 ± 0.05	—
	τ^{a} (ns)	1.07 ± 0.15	0.95 ± 0.2	1.0 ± 0.15	1.0 ± 0.2	—

^a Excitation wavelength $\lambda_{\text{exc}} = 380$ nm; observed wavelength $\lambda_{\text{obs}} = \lambda_{\text{e}}^{\text{max}}$.

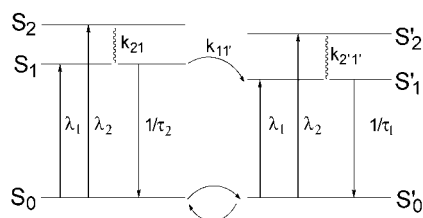


Figure 5. Spectroscopic model of **4**. S_i , electronic molecular levels of short-wavelength conformer ($i=0, 1, 2$) and long-wavelength conformer ($i=0', 1', 2'$); λ_j ($j=1, 2$), excitation wavelength; k_{lm} ($l=1, 2, 2'$; $m=1, 1'$), velocities of the radiationless transitions; τ_1 and τ_2 , lifetimes of S'_1 and S_1 , respectively

explained by the predominant excitation of the longer wavelength absorbing chromophore. The values of r were even lower [Fig. 4(a), curves 9–11] for low-viscosity solvents (hexane, THF and CH_2Cl_2), owing to the fast rotation of **4** in these solvents.

The values of the quantum yields, Φ , of **4** in hexane, THF and CH_2Cl_2 , for excitation in the maximum of the absorption band, λ_a^{max} , are near unity (Table 1). The quantum yields for **4** were consistently high and independent of the solvent. Taking into account the fast relaxation process $S_1 \rightarrow S'_1$, we can attribute the high values of Φ to the lower energy (longer wavelength) chromophore.

Fluorescence and excitation spectra of **4** in 2-methyltetrahydrofuran (Me-THF) at 77 K are presented in Fig. 6. The fluorescence emission spectra of **4** were independent of excitation wavelength in the spectral region $\lambda_{\text{exc}} \leq 400$ nm (curves 2 and 3). Emission spectra for $\lambda_{\text{exc}} > 400$ nm are presented in Fig. 7 and show a clear dependence on the excitation wavelength. In this case, the fluorescence spectra of the lower energy chromophore (curve 4) can be extracted, owing to the lower degree of spectral overlap with the higher energy chromophore at low temperature. As shown in Fig. 7,

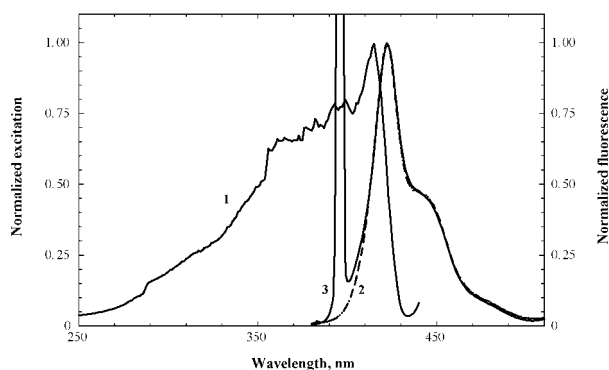


Figure 6. Normalized excitation (1) and fluorescence (2, 3) spectra for **4** in Me-THF at 77 K: 1, $\lambda_{\text{obs}} = 445$ nm; 2, $\lambda_{\text{exc}} = 300$ nm; 3, $\lambda_{\text{exc}} = 395$ nm (with scattering line on 395 nm)

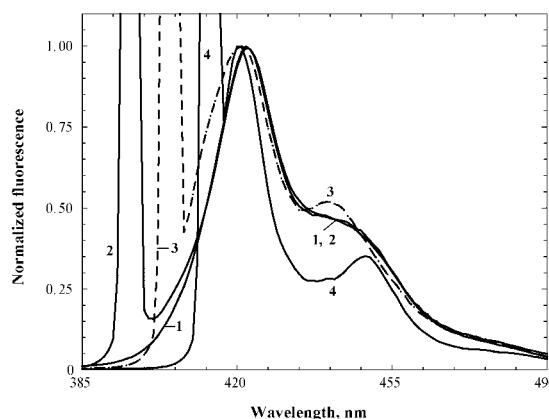


Figure 7. Normalized fluorescence spectra (1–4) for **4** in Me-THF at 77 K: 1, $\lambda_{\text{exc}} = 300$ nm; 2, $\lambda_{\text{exc}} = 395$ nm; 3, $\lambda_{\text{exc}} = 405$ nm; 4, $\lambda_{\text{exc}} = 415$ nm (curves 2–4 are shown with scattering lines)

the vibronic structure of the emission bands for the different chromophores is characterized by different spectral positions of the vibrational peaks. For $\lambda_{\text{exc}} = 415$ nm (predominant excitation of the lower energy chromophore) this peak is bathochromically shifted 6–8 nm relative to $\lambda_{\text{exc}} = 405$ nm. Compounds **4** and **5** were at least 99.6% pure, according to elemental analysis, hence any influence of impurities is unlikely.

Fluorescence decay of oligofluorene **4** at 77 K exhibited only one component, $\tau_1 \approx 1.55$ ns, which was independent of the wavelength of excitation. At low temperature, one can assume that the velocity of conformational reorientation of the higher energy chromophore, $k_{11'}$, after excitation to S_1 , was suppressed, resulting in the simultaneous independent emission of two conformers. This suggests that both conformers of **4** have similar fluorescence spectra and lifetimes at low temperature and emitted simultaneously.

The solid-state luminescence of a spin-cast thin film of neat **4** is shown in Fig. 8 along with absorption and emission in hexane solution. As expected for a concentrated or neat sample, the emission spectrum is red shifted but maintains the general spectral features of the solution-phase spectrum. The thin solid film of **4** exhibited bright fluorescence emission from 425 to 470 nm.

CONCLUSION

A well-defined, blue light-emitting, oligofluorene derivative (**4**) was prepared via relatively efficient Ullmann condensation methodology. It was found that this compound is amorphous and stable up to nearly 400 °C under N_2 . Cyclic voltammetric measurements showed that this compound possesses low oxidation potentials and high electrochemical stability, even after repeated redox cycles in CH_2Cl_2 . Oligofluorene **4**, in addition to

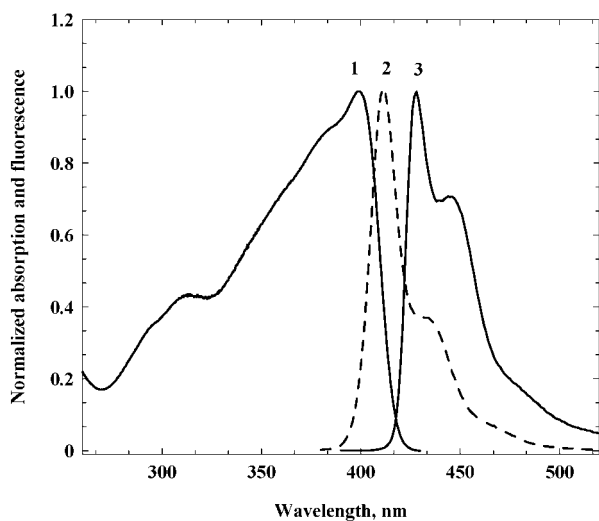


Figure 8. Normalized absorption and fluorescence spectra (1–3) for fluorene **4** at room temperature: (1) absorption in CH_2Cl_2 ; (2) fluorescence in CH_2Cl_2 ; (3) photoluminescence of neat thin film

servicing as a potential model compound for luminescence materials development, allowed the spectroscopic study of multiple chromophores in a single molecule. The absorption and fluorescence spectra of **4** exhibited a weak dependence on solvent polarity and an insensitivity to the number of fluorene units in the molecule. The fluorescence spectra of **4** were independent of the excitation wavelength over a range of solvents at room temperature. Excitation anisotropy spectra and the detection of two components in the fluorescence decay of **4** at room temperature suggested a different orientation of the end fluorenyl chromophores in **4** relative to the central fluorene core, and a fast reorientation process upon excitation.

At low temperature (77 K), the emission spectra of different chromophores within the molecule (the lower energy chromophore in particular) were resolved under excitation at the red edge of the absorption band. The fluorescence decay at 77 K was characterized by single exponential process and was independent of the excitation wavelength, indicative of a decrease in the velocity of chromophore reorientation and simultaneous emission of the various conformers.

As a result of this investigation, it can be concluded that the general steady-state fluorescence properties will be nearly independent of the number of fluorenyl units in a molecule. For example, in a polymer with aminofluor-

enyl repeat units, the spectral behavior is expected to be similar to that of the individual repeat unit, thereby affording valuable design rationale, an aspect under further investigation. Oligofluorene **4** exhibited bright blue luminescence in both the solid state and solution. In solution, the fluorescence quantum yield was near unity, further suggesting the strong potential of oligofluorene **4** as an emissive material for OLEDs.

Acknowledgements

We acknowledge the donors of the Petroleum Research Fund of the American Chemical Society, Research Corporation (Cottrell College Science Award), the National Science Foundation (DMR-9975773, ECS-9970078 and ECS-9976630), the National Research Council (COBASE) and the University of Central Florida (Presidential Research Equipment Initiative) for support of this work.

REFERENCES

- Sogulyaev YuA, Mushkalo IL, Tolmachev AI. *Ukr. Khim. Zh.* 1992; **58**: 265–268.
- Chen JP, Klaerner G, Lee JI, Markiewicz D, Lee VY, Miller RD, Scott JC. *Synth. Met.* 1999; **107**: 129–135.
- Morel Y, Irimia A, Najechalski P, Kervella Y, Stephan O, Baldeck PL. *J. Chem. Phys.* 2001; **114**: 5391–5396.
- Kim DY, Cho HN, Kim CY. *Prog. Polym. Sci.* 2000; **25**: 1089–1139.
- Kiprianov AI. *Usp. Khim.* 1971; **40**: 1283–1308.
- Ibrayev NK, Ishchenko AA, Karamysheva RKh, Mushkalo IL. *J. Lumin.* 2000; **90**: 81–88.
- Chibisov AK, Zakharova GV, Gorner H, Sogulyaev YuA, Mushkalo IL, Tolmachev AI. *J. Phys. Chem.* 1995; **99**: 886–893.
- Belfield KD, Schafer KJ, Mourad W, Reinhardt BA. *J. Org. Chem.* 2000; **65**: 4475–4481.
- Belfield KD, Hagan DJ, Van Stryland EW, Schafer KJ, Negres R. *Org. Lett.* 1999; **1**: 1575–1578.
- Bliznyuk VN, Carter SA, Scott JC, Klarnar G, Miller RD, Miller DC. *Macromolecules* 1999; **32**: 361–369.
- Belfield KD, Bondar MV, Przhonska OV, Schafer KJ, Mourad M. *J. Lumin.* 2002; **97**: 141–146.
- Belfield KD, Bondar MV, Przhonska OV, Schafer KJ. *J. Fluoresc.* 2002; **12**: 445–450.
- Lakowicz JR. In *Principles of Fluorescence Spectroscopy*, Kluwer Academic/Plenum: New York, 1999; 52–53, 298–300, 648.
- Fischer M, Georges J. *Chem. Phys. Lett.* 1996; **260**: 115–118.
- Belfield KD, Schafer KJ, Alexander MD Jr. *Chem. Mater.* 2000; **12**: 1184–1186.
- Yavuz O, Sezer E, Sarac, AS. *Polym. Int.* 2001; **50**: 271.
- Baur JW, Alexander Jr MD, Banach M, Denny LR, Reinhardt BA, Vaia RA, Fleitz PA, Kirkpatrick SM. *Chem. Mater.* 1999; **11**: 2899–2906.